/JS

PS / LP Note 91-01
20 février 1991

Results from the First Power Tests of the RF Gun Foreseen as Electron Source in the CTF

R. Bossart

B. Canard

J.-Cl. Godot

H. Kugler

G. Rossat

J. Stroede

(November 1990)

Results from the first power tests of the RF gun foreseen as electron source in the CTF

R.Bossart, B.Canard, J.C.Godot, H.Kugler, G.Rossat, J.Stroede

November 27, 1990

1 Introduction

The 2nd BNL type RF gun (gun-II, fig.1) for the CTF has been brought into experimental stage in week 43. Unlike its predecessor (gun-I) it was designed to be pumped, tuned and then powered up to its nominal pulse power of 6MW/2.5μs. However, this version did not make use of a special cathode material nor laser illumination. Only the cathode support made of copper OFHC was put in. After installation in a temporary position in the CTF blockhouse and a series of low power tests the first vacuum and RF conditioning followed. During that period measurements of the dark current delivered by the gun were performed using a Faraday cup (fig.2).

2 RF processing

The gun was powered by Klystron MDK 97 in the LIL gallery via a waveguide network (sharing the power by a 3db hybrid with a dummy load, fig.3). Prior to the power tests, the gun was tuned for it's operational frequency 2998.5 MHz with the cavity under vacuum and with a cooling water temperature of 30.0 ± 0.1°C. It was tuned for equal field strength in both cells. The matching of the waveguide to the cells was rather sensitive to the amplitude ratio E_1/E_2 (E_1 = the max. field strength at the cathode, E_2 = max. fieldstrength on axis in the 2nd cell). This ratio, the resonance frequency, and the matching were checked with a network analyser (fig.4).

After these low power tests, the gun was baked out at about 120°C during 24 hours. Since multipactoring was expected in the gun at a very low power level, the RF processing started already with a few kW. Effectively, multipactoring took place between 50kW and 100kW at the gun input and was overcome after a day of RF processing. In another day the power could be raised easily to 1MW, under normal outgasing conditions. Above this power level outgasing became stronger and sparking happened frequently. Therefore the pulse duration of the klystron was reduced from 4μs to 2μs. From now on the RF processing became slower. A barrier was hit between 2MW and 4MW. It could be overcome after a week. Within a 2nd week the nominal power of 6MW was reached. The vacuum pressure in the gun had raised from 3×10^{-10} Torr for 4MW to 3×10^{-9} Torr for 6MW. The pressure was measured by a calibrated gauge mounted on the pumping manifold on the waveguide at the gun input.

The power of klystron MDK97 was measured by a peak power meter via a directional coupler 60/54db on the waveguide at the output of the klystron. The calibration of this equipment and the insertion loss of the waveguides and the power splitter provide the ratio of the klystron output power measured with the peak power meter and the power at the input of the gun (equation (3) below). Fig.5a shows the waveform of the klystron with strong ripple on the klystron voltage. The exponential filling of the standing wave cavity and it's discharging is shown by a probe signal from the $\lambda/4$ cell, measured by the automatic peak power meter, fig.5b. The power reflected by the gun is shown in fig.5c.

3 Measurement of the integrated dark current

For the measurement of the integrated dark current spare parts from our photocathode lab were used to build a Faraday cup [1]. Since electrons with energies up to about 4MeV were expected the cup was modified joining the collector with a long cylinder made out of aluminium. In order to use the cup as an independent measuring unit it was equiped with a separate pumping system. The new layout is given in fig.6. Two different types of entrances, flange with tube (FWT) or without tube (FTL) were used (fig.7) providing different particle admittances. A chain of preamplifier with current integrator, sample

and hold, and amplifier was used to produce a voltage signal to be processed then by a ADC. The sample and hold unit was triggered by the klystron (10Hz), the sample is taken with an internal delay of about 6μs and then hold for about 16ms.

It was foreseen to measure the integrated dark current delivered by gun-II as a function of the electric field (Fowler-Nordheim relation, [2]). Putting successively aluminium absorbers of different width into the beam the practical range of the electrons and hence their energy [3] was also expected to be measured within the whole range of peak field strengths at the cathode E_{cat}. Due to stability problems of the klystron as well as the amplifier/integrator circuits used, only some series of the planed measurements could be done. Those were performed using different geometries and the two different front end windows (FWT, FTL).

Fig.9 shows the integrated dark current Q measured with the FWT in position DG = 0, i.e. the Faraday cup installed as near as possible to the the gun (fig.6). The charge is plotted as a function of the peak surface field E_p in a Fowler-Nordheim diagram. The slope of the resulting, nearly linear curve is proportional to $1/\beta$, where β is the so-called field enhancement factor. It gives an estimate of the 'local' peak field in a high gradient structure ($E_{p,local} = \beta \times E_p$). Thus it is a measure of the surface quality [2]. We found a β-factor of about 100 (using as workfunction for copper ϕ = 4.65eV; [4]) a Q in the order of 16nC at E_p = 136MV/m by extrapolation from measurements at lower E_p.

Using the same setup we measured Q as a function of DG. The power at the output of the klystron was P_{klys} = 7MW. On a logarithmic scale one finds a linear curve as given in fig.10. Extrapolation to negative values of DG which is equivalent to approaching the detector to the outlet of the gun (DG = -12cm) indicates that the total charge leaving the gun is 3 times the value measured at DG = 0. Even though it was impossible to derive the angular distribution of the beam on the basis of these measurements, this factor became important for the evaluation of the experiments described below.

Only one measurement of the total dark current at a field E_{cat} = 100MV/m could be performed, that one in configuration FTL, the detector at DG = 0. 15nC are found (fig.11). This agrees well with the 16nC from extrapolation (see fig.9). The charge leaving the gun at the outlet window is then 3×15nC = 45nC per rf pulse (2μs) i.e. 10pC / rf cycle, using the factor 3 explained before. The corresponding 'peak' dark current is about a factor 6 higher than the 'mean' current since the field in the gun varies sinusoidally. Transfering the data of fig.11 in a Fowler-Nordheim plot shows a β-factor comparable to the value found at the beginning of formation (fig.12).

TBCISF simulations of the beam dynamics in the gun [5] have shown that the mean photo current produced by nanosecond light pulses of a Nd:YAG laser can reach 2.2nC / rf cycle at photocathode quantum efficiencies of some 10^{-5} as assumed for the calculations. In that case the ratio of photo current to dark current (mean values) would be about 200.

At BNL, for a very similar rf condition, about 80pC were measured (fig.16). This is not in discrepancy with our results as at BNL the measurement was restricted to particles with the maximum energy and an energy dispersion of less than ±2% thanks to their spectrometer magnet.

4 Measurement of the max. kinetic energy

Simulations using TBCISF have shown [6] as rough law for the peak kinetic energy T_{th} as function of the field E_{cat}:

(1) $$T_{th} = E_{cat}/25$$ where $[T_{th}]$ = MeV and $[E_{cat}]$ = MV/m.

URMEL calculations predict a gun input power P_{gun} = 6MW to create a field E_{cat} = 100 MV/m in gun-II. It follows that:

(2) $$E_{cat} = 100 \times \sqrt{P_{gun}/6}$$ where $[P_{gun}]$ = MW.

The total attenuation of the network is about -4.2db, so:

(3) $$P_{gun} = 0.38 \times P_{klys}$$ where $[P_{klys}]$ = MW.

Table 1 summarizes P_{gun}, E_{cat}, E_p, and T_{th} for different klystron powers.

For any absorber material of the density ρ an empirical law relates the penetration depth R, called practical range, to the peak energy T_{ex} of the electron beam:

(4) $$R \times \rho = 0.53 \times T_{ex} - 0.106$$ where $[T_{ex}]$ = MeV, $[R]$ = cm, and $[\rho]$ = g/cm^3.

One should note that this empirical law has a poor accuracy of some percent for a range of the kinetic energy of 1 - 30MeV. Fig.13 shows a typical plot of detected electrons as function of the width of the absorber. It shows how to derive R from the values measured.

For our case we used aluminium discs of the width 1 mm as absorbers. This gave an energy resolution of about 0.5 MeV as can be seen from (4). The measurements for P_{klys} = 7MW and 15MW are given in the figures 14 and 15. Because of the technical problems mentioned before the measurement at P_{klys} = 15MW does not allow a good estimate of T_{ex}. The experimental values of the kinetic energies T_{ex} are given in table 1. It should be mentioned that the charge measured without absorber is a factor of 1000 higher than the charge created by gamma radiation. The latter is measured as a background when using a sufficiently thick absorber (fig.13, 14 and 15).

5 References

(1) "Coupe de Faraday", Y.Pellegrina, PS/LP note 89-20, August 1989.
(2) "Progress report on high-gradient rf studies in copper accelerator structures", G.A.Loew and J.W.Wang, SLAC-PUB-5320, September 1990.
(3) "Range-Energy Relations for Electrons and the Determination of Beta-Ray End-Point Energies by Absorption", L.Katz and A.S.Penfold,Rev.Mod.Phys. 24, pp.28-44, (1952).
(4) "Field emission and rf break down in copper linac structures", G.A.Loew and J.W.Wang, Particle Accelerators, vol.30, pp.225-230, (1990).
(5) "Beam dynamics of trains of bunches from very long laser pulses in the CTF rf gun", H.Kugler, J.Stroede, PS/LP note 90-36, August 1990.
(6) "Catalogue of simulations of the CTF rf gun", J.Stroede, PS/LP note 90-35, August 1990.

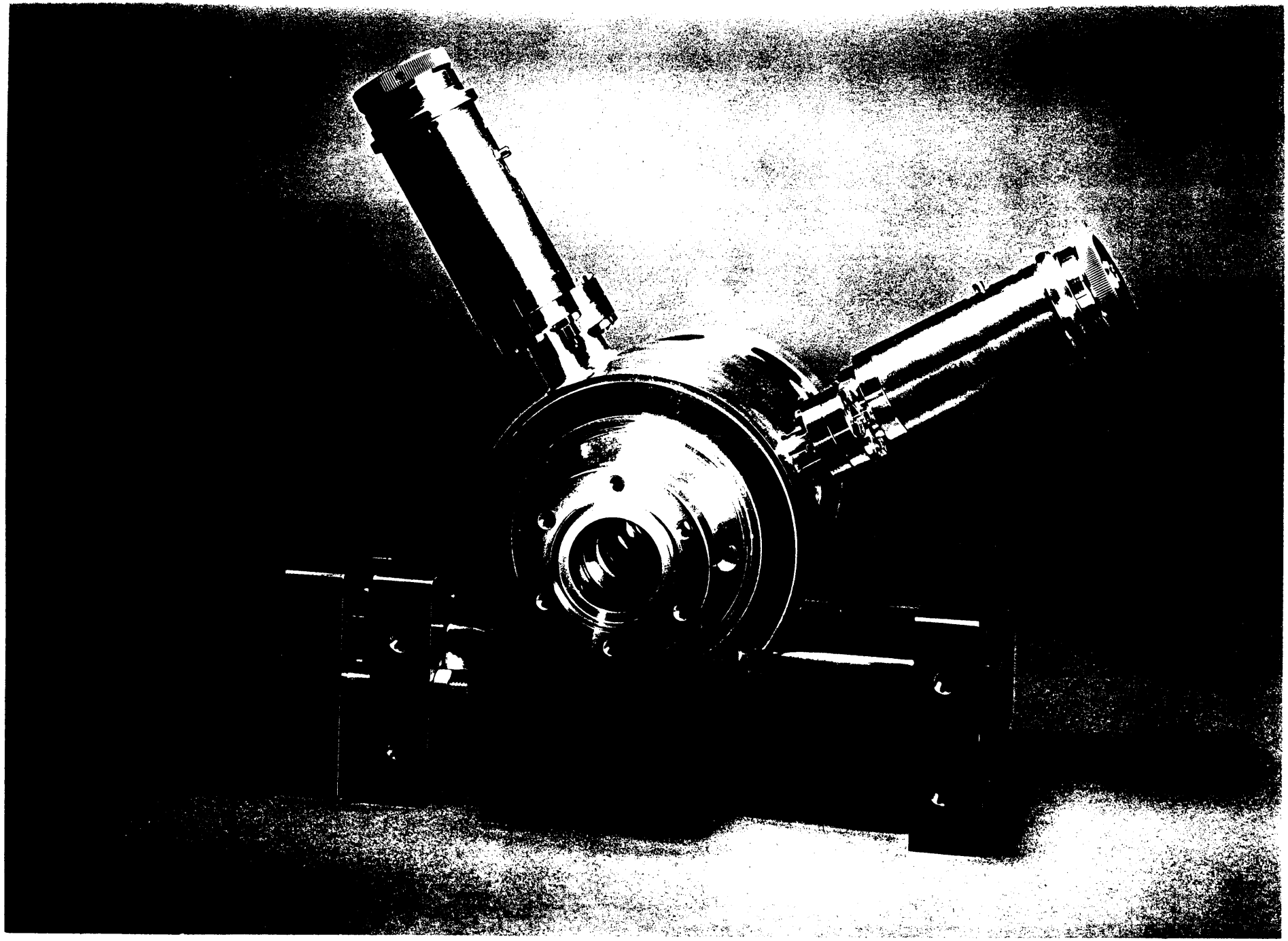

Fig. 1: The CTF rf gun with waveguide and tuners.

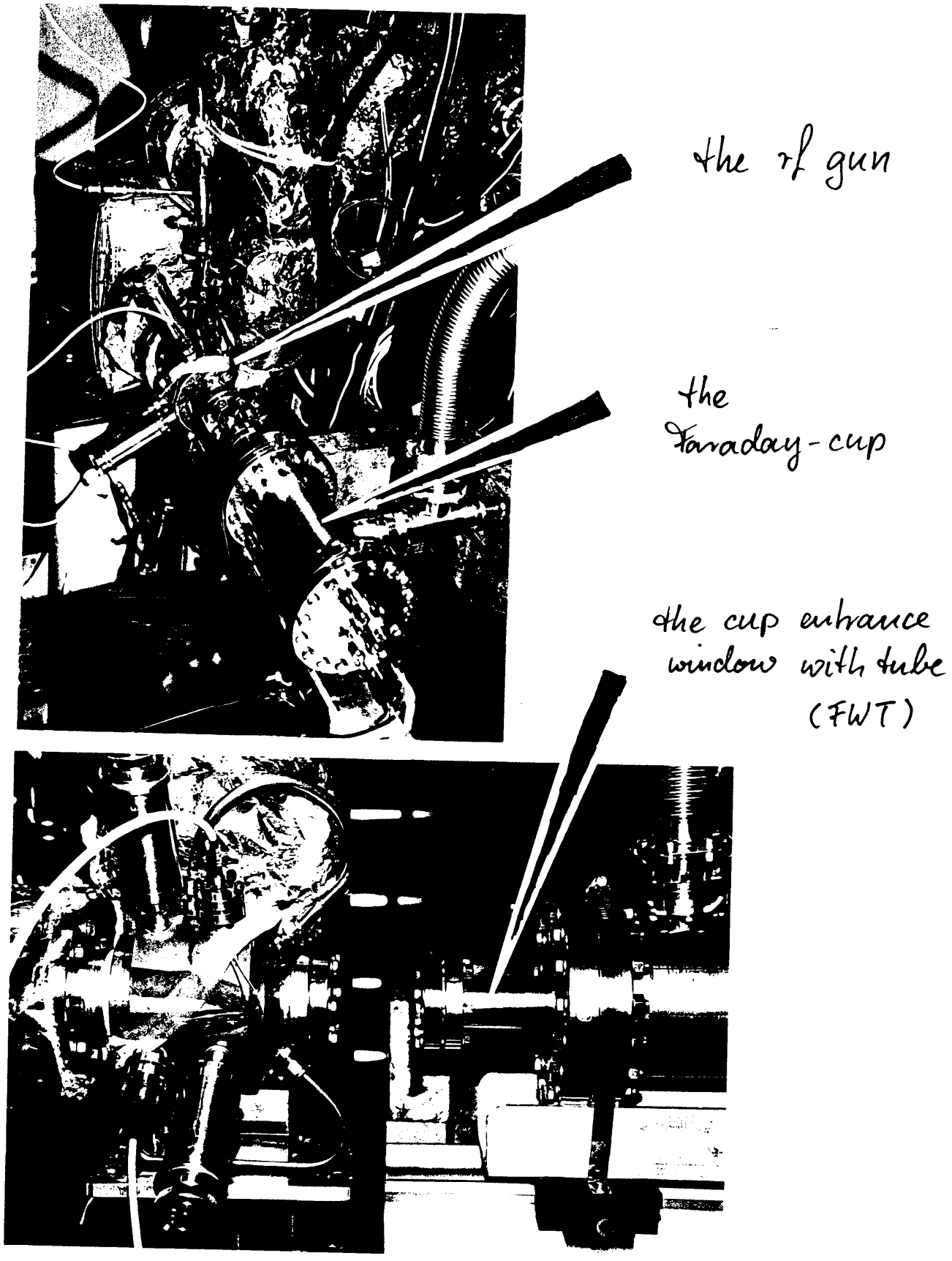

Fig. 2: The CTF test stand with rf gun and Faraday cup in week 43 (1990).

Table 1:

P_{klys}	2	4.5	7	15	16	Output power of the Klystron [MW]
P_{gun}	0.8	1.7	2.7	5.7	6.1	Input power at the gun [MW]
E_p	47	71	89	129	136	Peak surface field [MV/m]
E_{cat}	35	52	65	95	100	Electric field at the cathode [MV/m]
T_{kin}	1.4	2.1	2.6	3.8	4.0	Calculated max. kin. energy [MeV]
T_{ex}		1.9	2.5	3.5-4.8		Max. kin. energy derived from Feather laws [MeV]

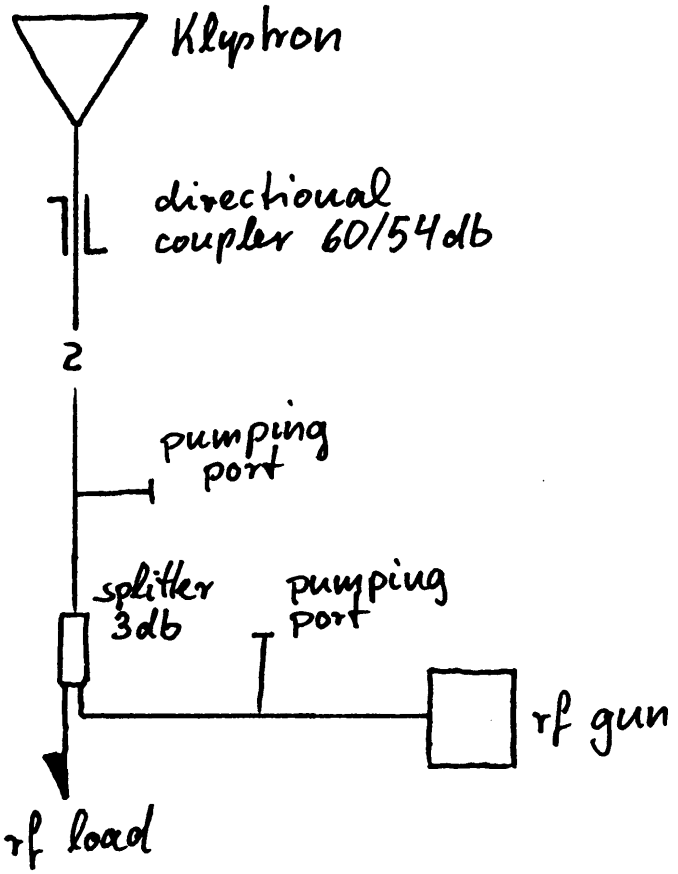

Fig. 3: RF power distribution in the CTF in week 43.

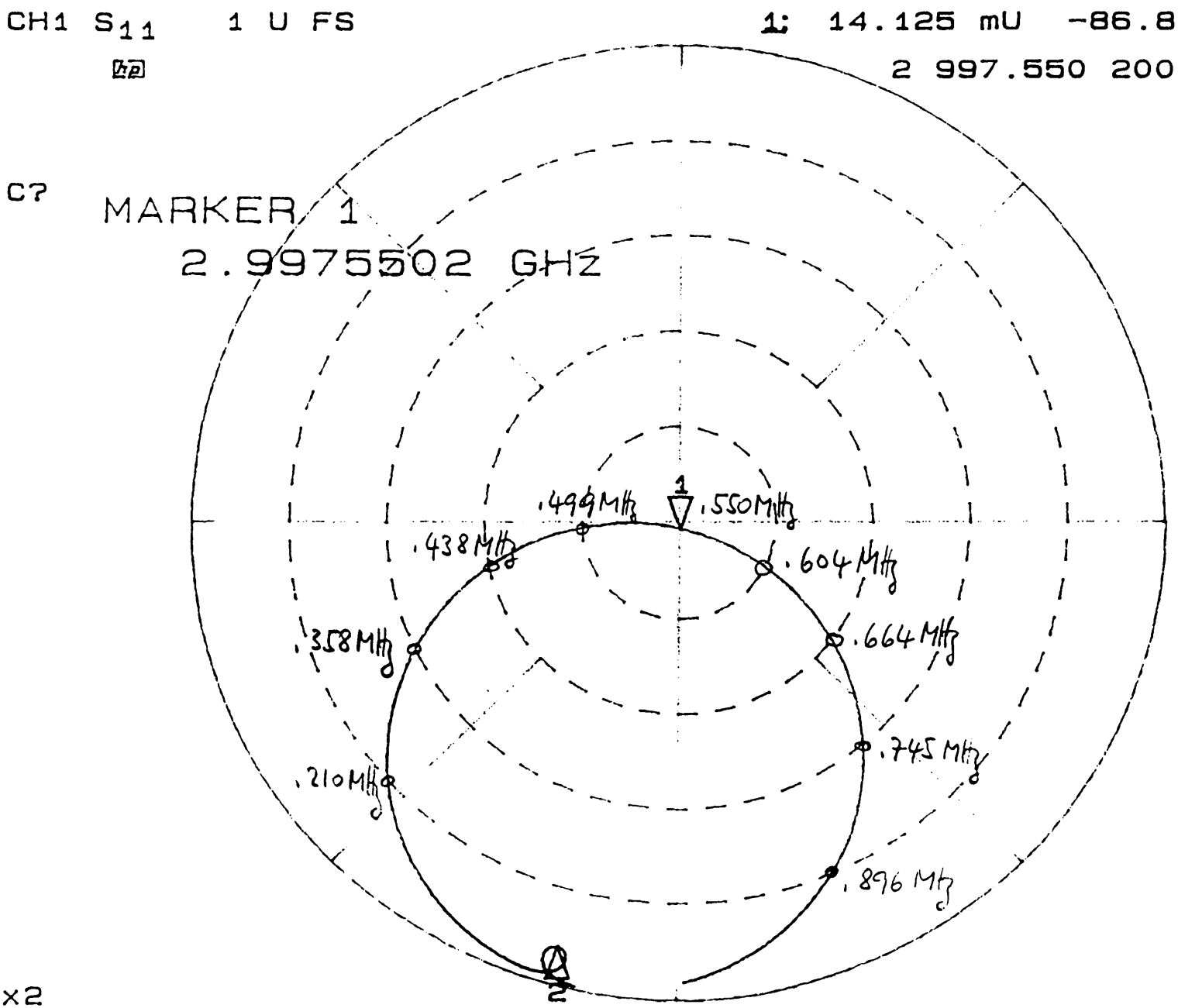

RF - Gun II

water cooled 30.0°C

$f_1 = f_\pi = 2997.550$ MHz

$r_1 = 0.014$, VSWR = 1.03

$f_2 = f_0 = 2995.537$ MHz

$r_2 = 0.928$

Tuner A

31.86 - 29.35 = 2.51 mm

Tuner B

31.20 - 29.50 = 1.70 mm

T = 22.5° C air

H = 54 %

P = 764 mbar

28.9.90

FIG. 4: Tuning and Matching of RF - Gun

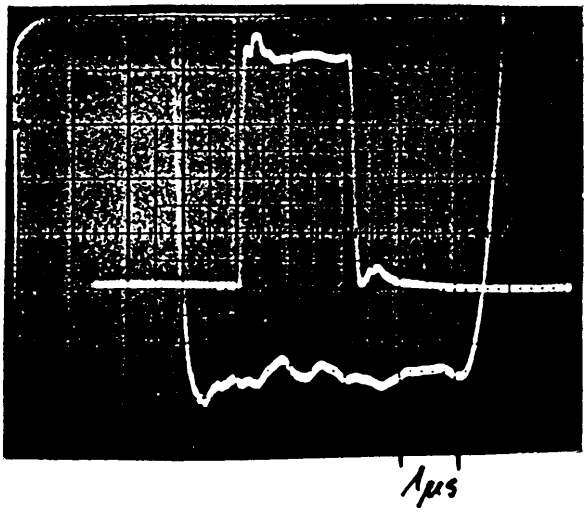

Fig 5a:
from klystron MDK 97
pos. pulse: 2µs rf-pulse
(14 MW, 3.25 MW/div)
neg pulse: 5µs cathode pulse
(234 kV, 1.8 kV/div)
modulator ripple ~ $6 \cdot 10^{-3}$

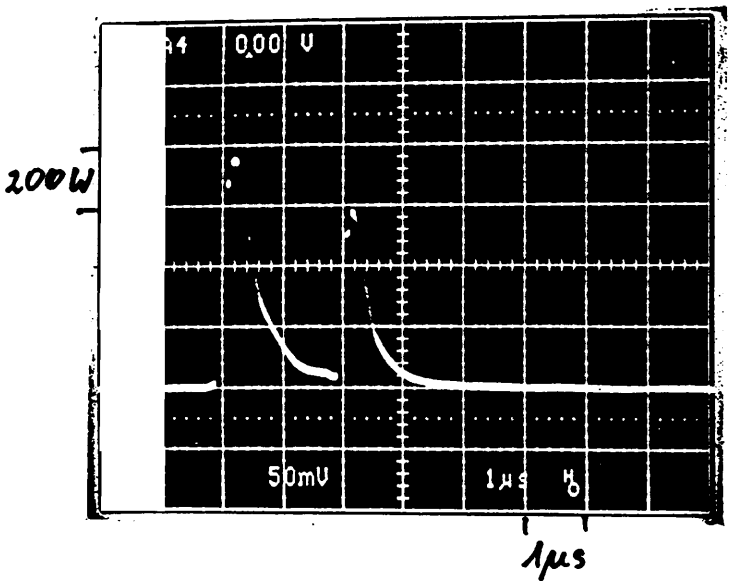

Fig 5b:
reflection from rf-gun;
note the small
mismatch after 2µs

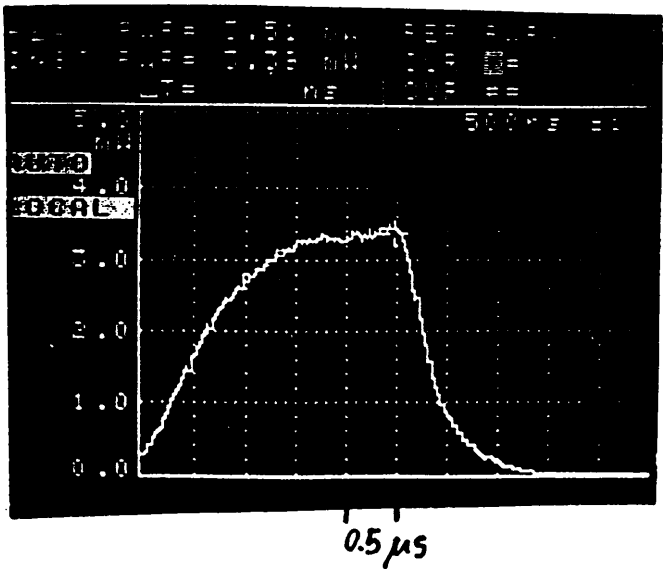

Fig 5c:
rf power in the gun
measured by loop PL1:
P= 0.38 MW × PL1/mW

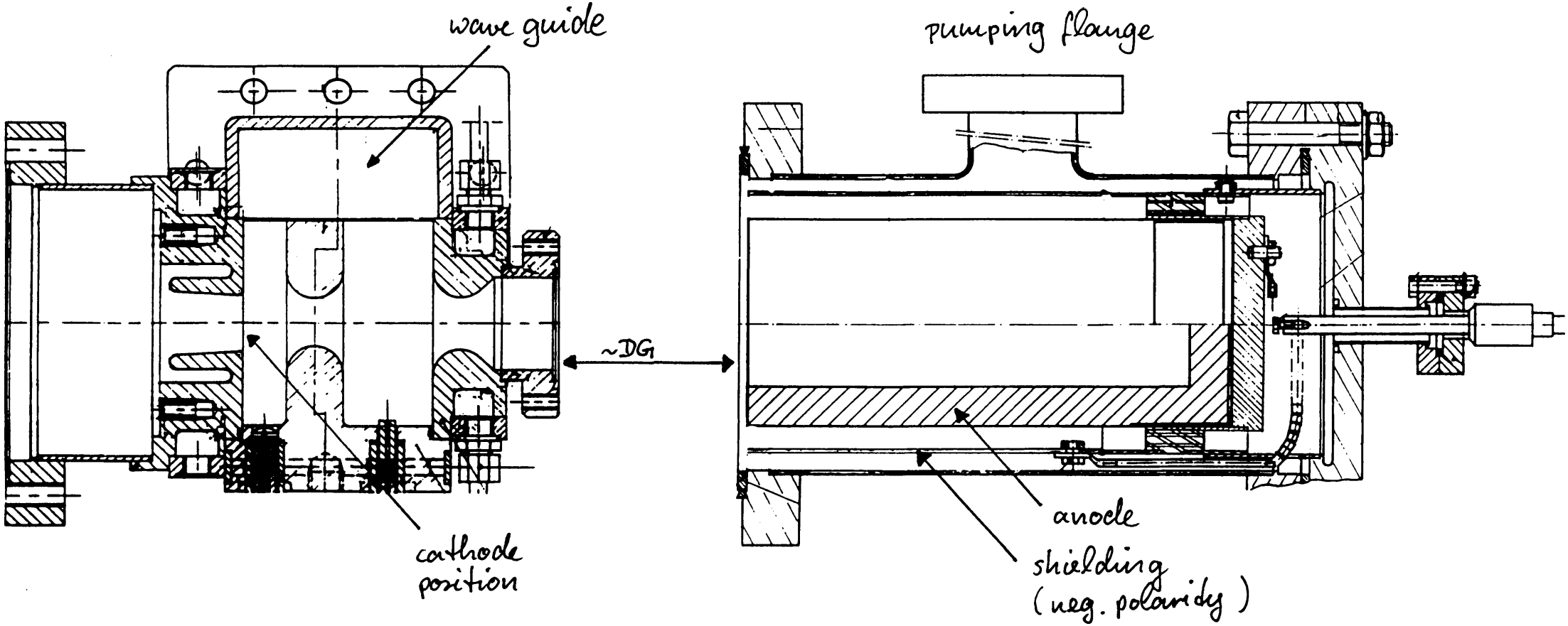

Fig. 6: Section of the rf gun and the Faraday cup.

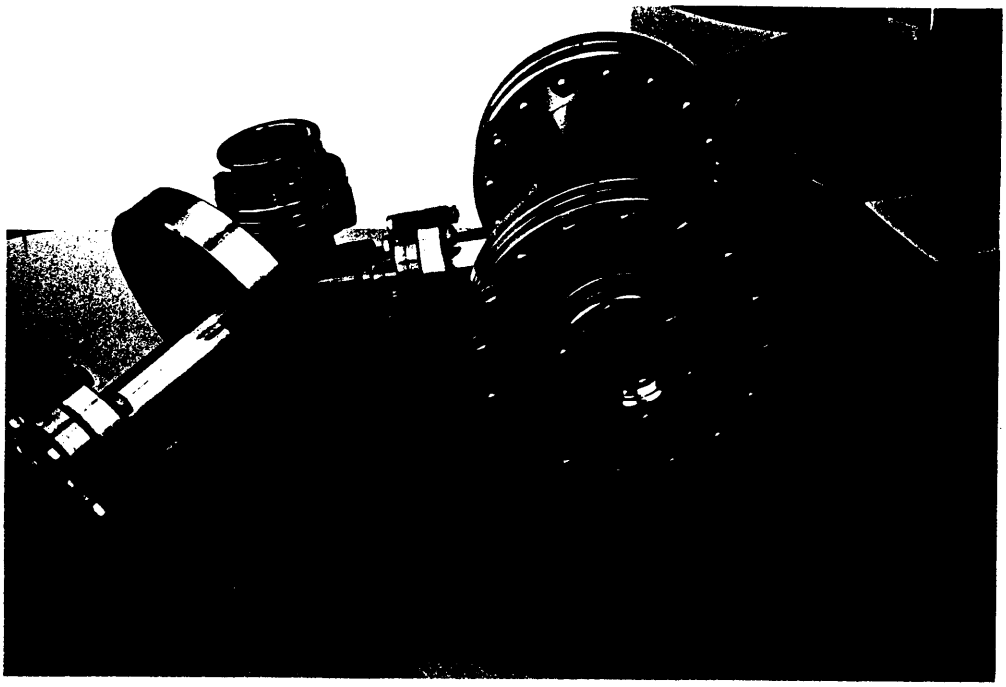

Fig. 7: The Faraday cup (short front end window for max. beam admittance installed), and the long front end window.

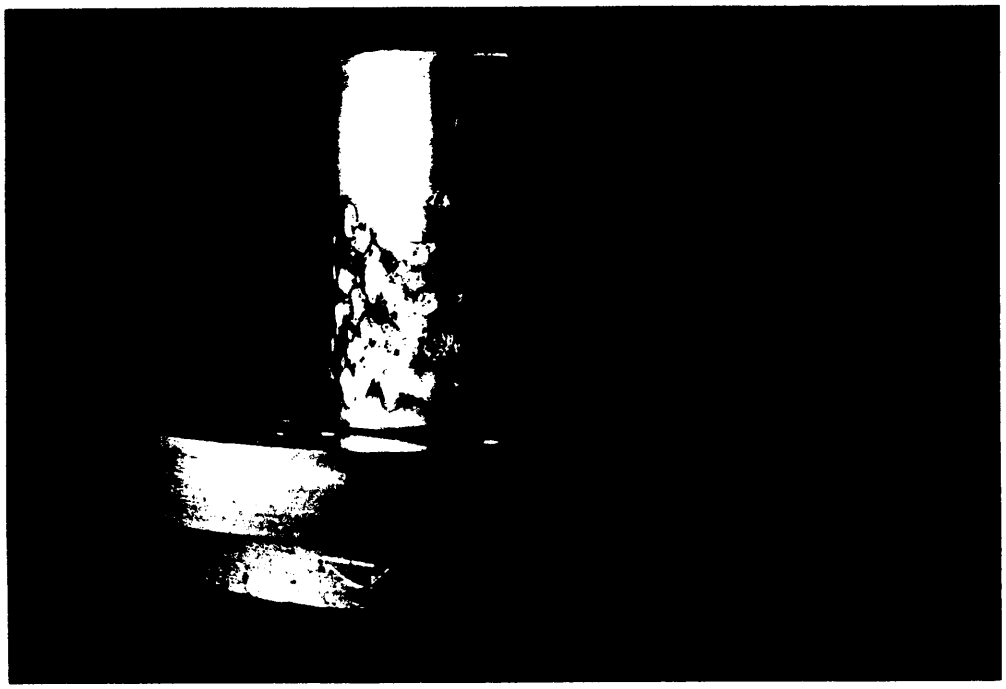

Fig. 8: The cathode plug after formation of the rf gun up to a peak surface field E_p = 136 MV/m.

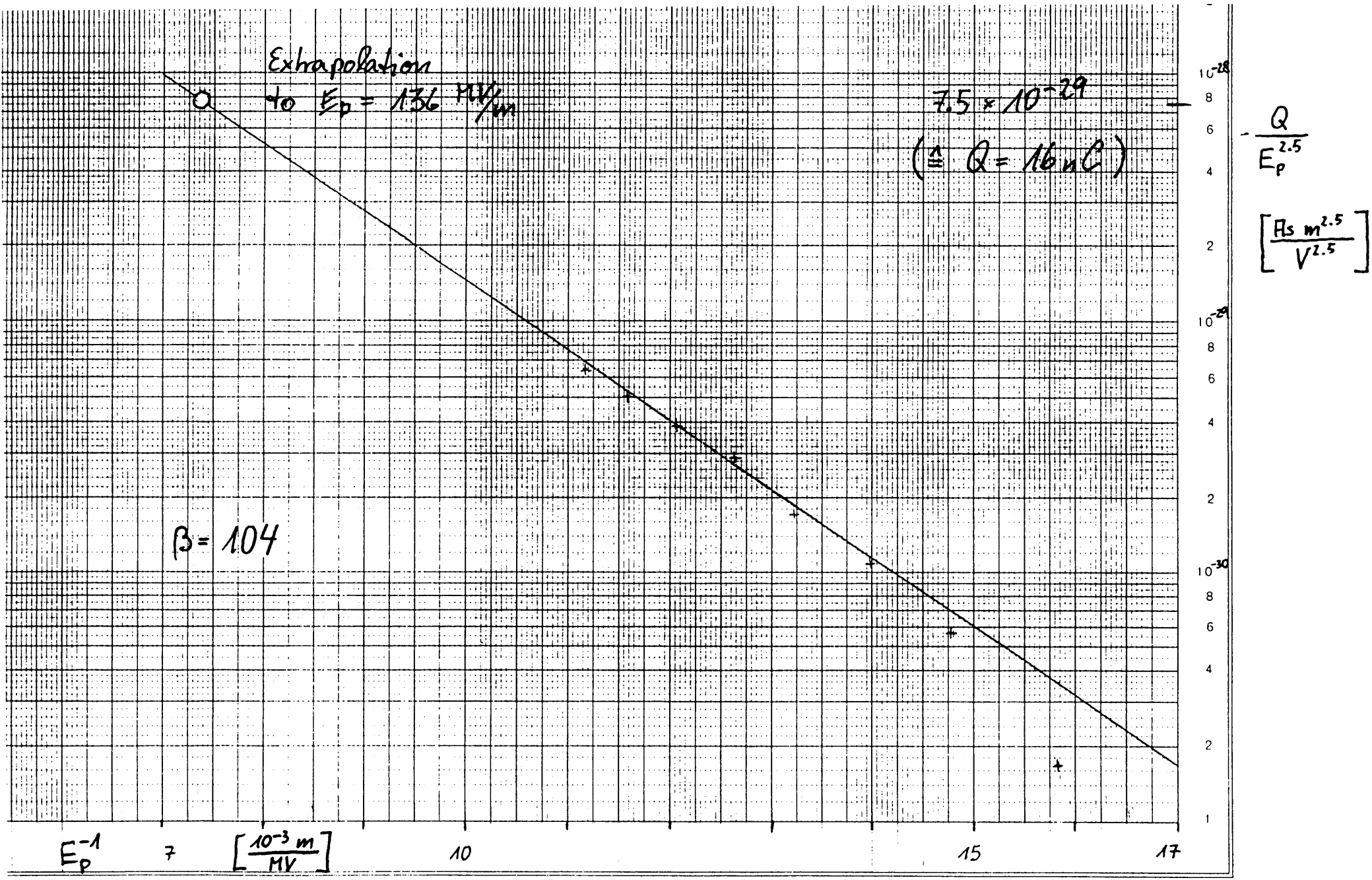

Fig. 9: Charge Q from dark current versus peak surface field E_p at low input power at the beginning of the formation process.

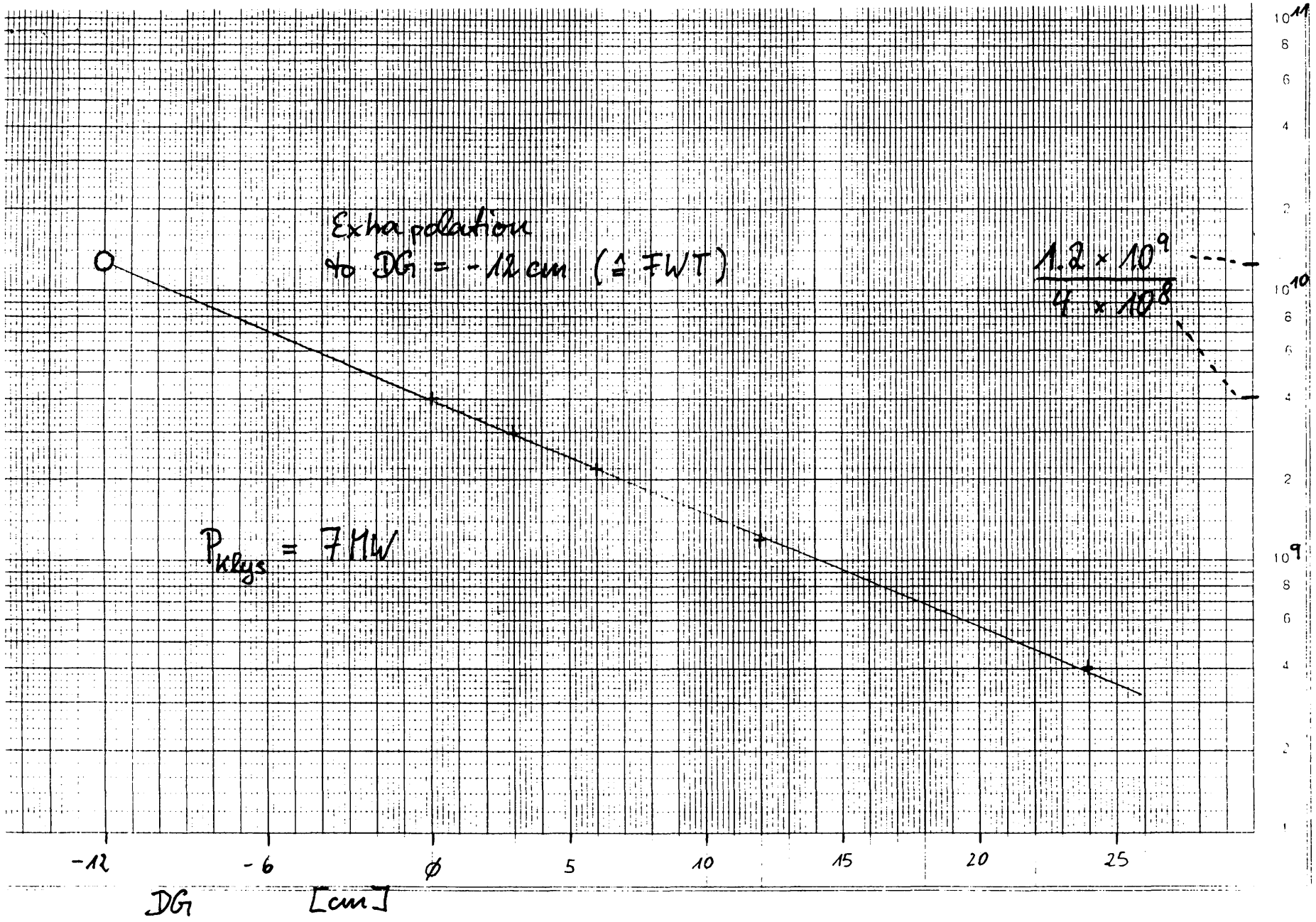

Fig. 10: Charge Q from dark current versus longitudinal distance cup-to-gun DG at low input power at the beginning of the formation process.

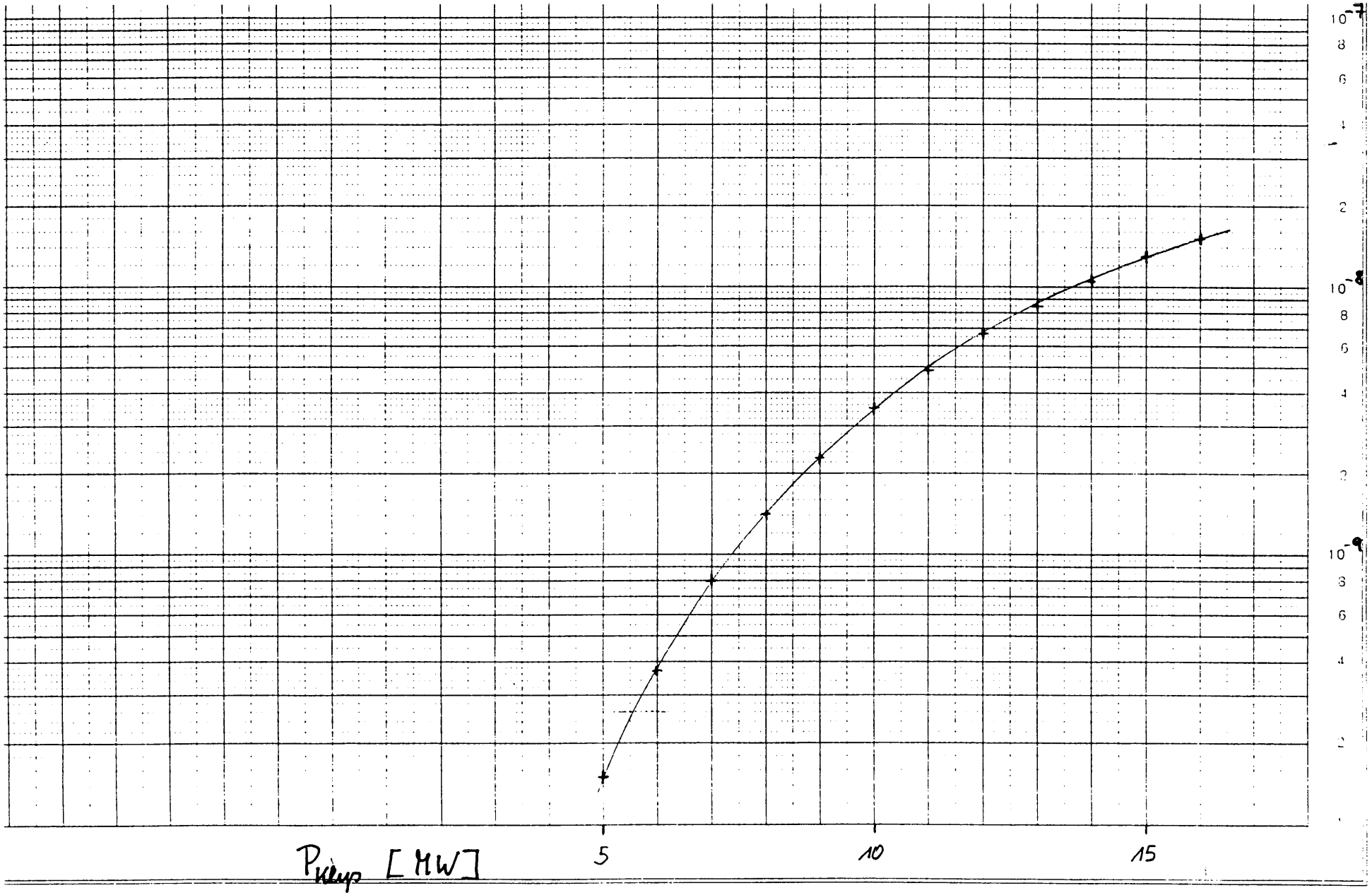

Fig. 11: Charge Q from dark current versus klystron output power P_{Klyp} at the end of the formation process.

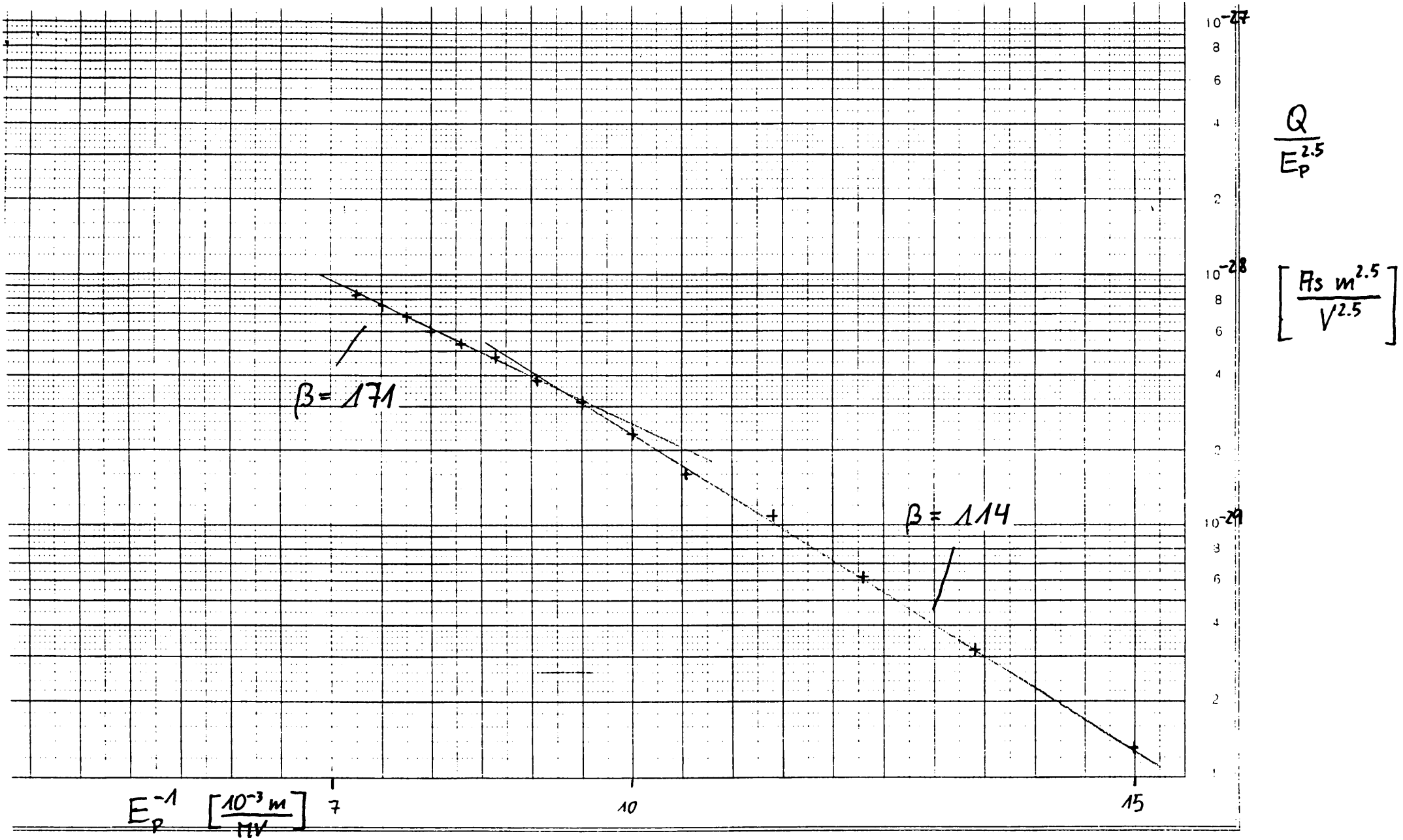

Fig. 12: - Charge Q from dark current versus peak surface field E_p at the end of the formation process (beta - plot).

kinetic energy of electrons as a function of the absorber-width

Absorption-law:

$$R_\varrho = 0.53 \times T_{ex} - 0.106$$

R - practical range of the e^- [cm]

ϱ - density of the absorber [g cm^{-3}]

T - kinetic energy of the e^- [MeV]

$\frac{\Delta T}{T} \sim 2\%$ for

$1\,MeV < T < 30\,MeV$

where R is to be found plotting the number of counts versus absorberwidth w

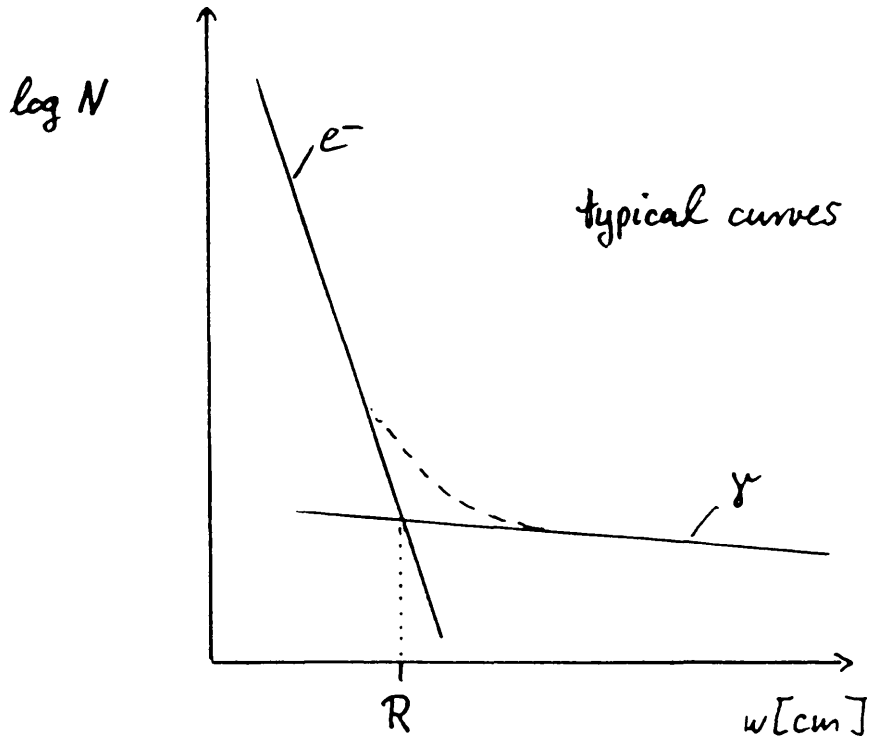

Fig. 13

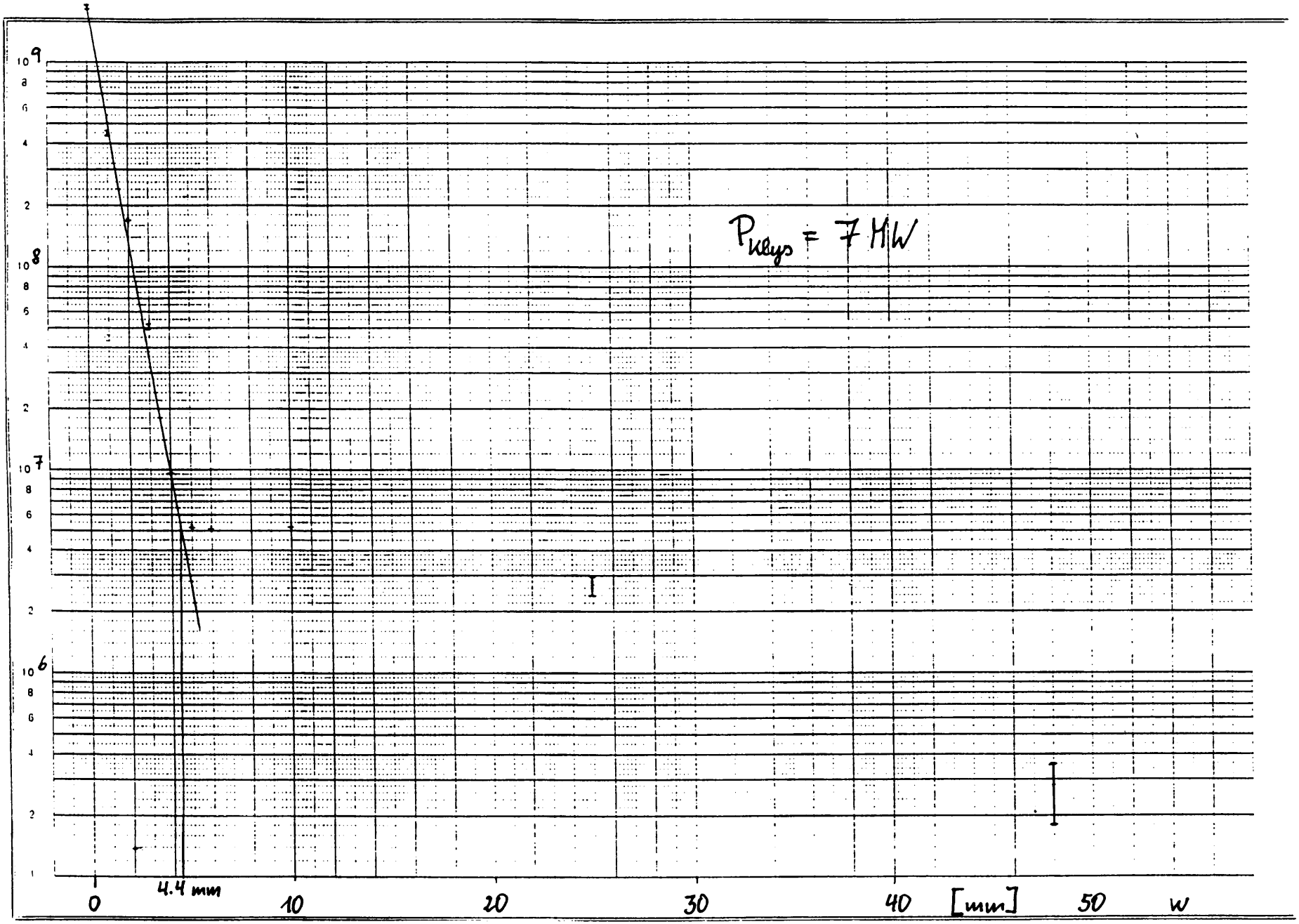

Fig. 14 : Charge Q from dark current versus absorber width w at $P_{Kly.} = 7$ MW.

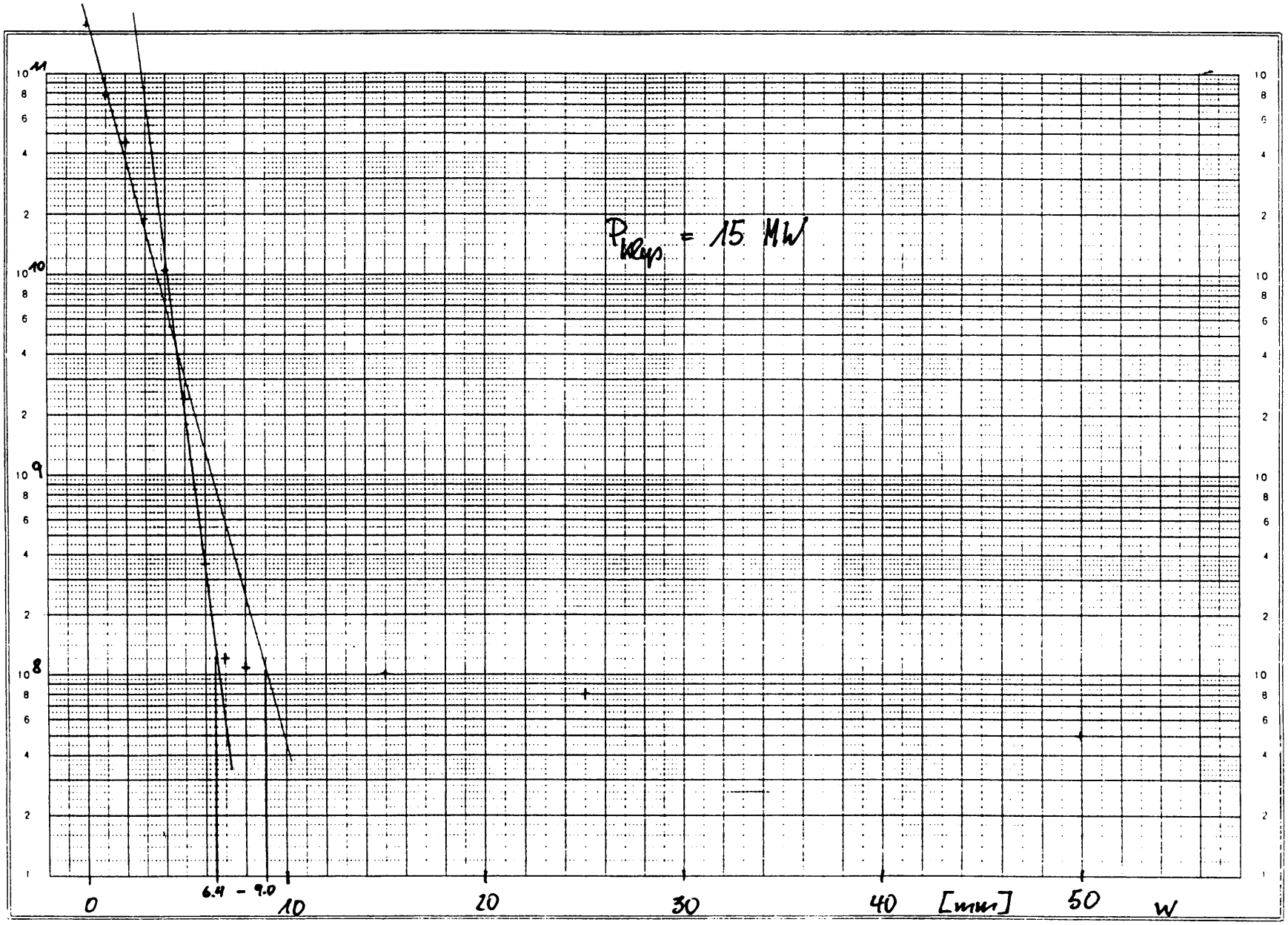

Fig. 15: Charge Q from dark current versus absorber width w at P_{klyn} = 15 MW.

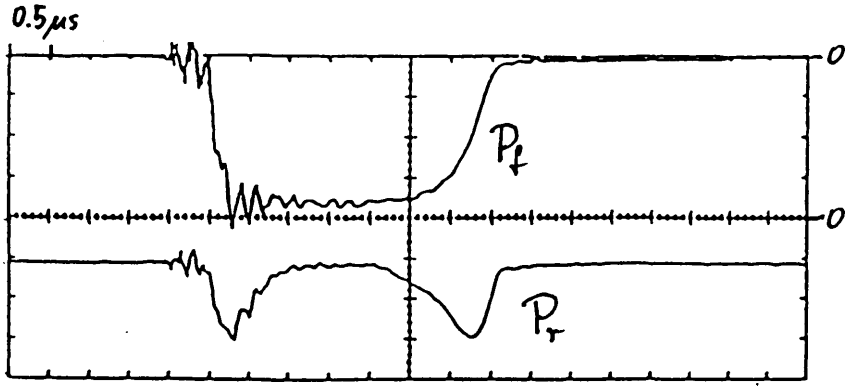

Forward and reverse power at the input to the rf gun.

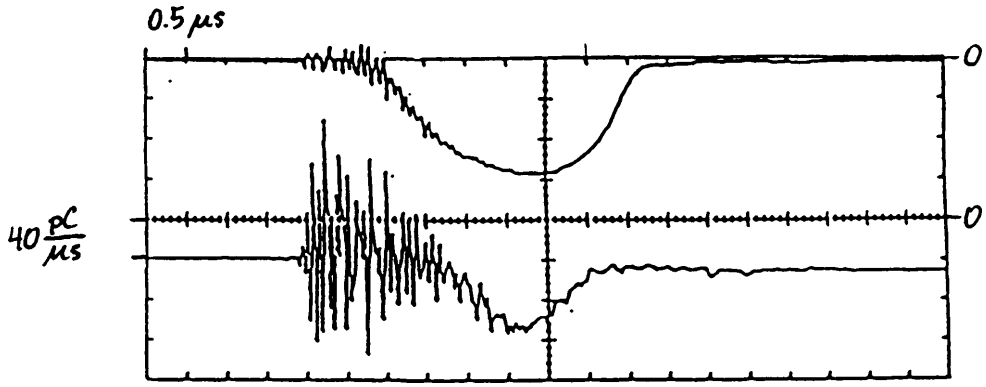

Gun cavity signal and Faraday cup signal measured into 50 Ω.

Tanabe, KEK, Lin. Coll. Workshop April 1990

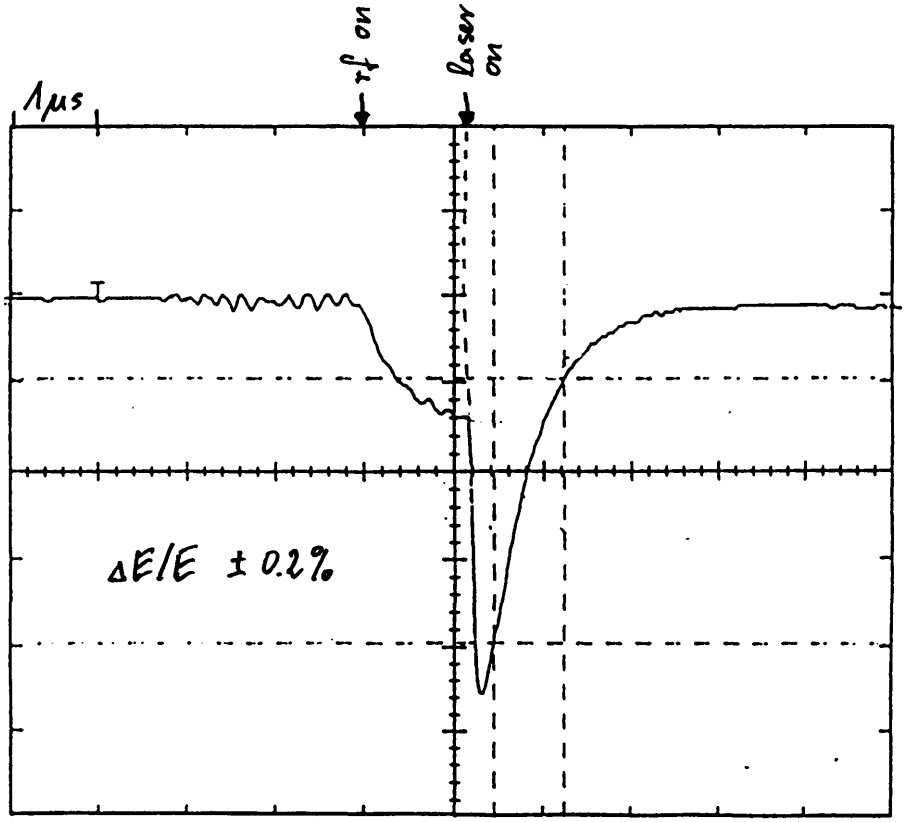

Dark current + photocurrent (laser: 600 μJ, 20 ns; $\eta = 1.4 \times 10^{-4}$)

Kirk, Erice Workshop April 1990

Fig. 16: Some results from measurements in the BNL Accelerator Test Facility.